Region Growing for Segmenting Green Microalgae Images

Vinicius R. P. Borges, *Member, IEEE,* Maria Cristina F. de Oliveira, *Member, IEEE,* Thaís Garcia Silva, *Fellow, OSA,* Armando Augusto Henriques Vieira, *Fellow, OSA,* Bernd Hamann, *Member, IEEE,*

Abstract—We describe a specialized methodology for segmenting 2D microscopy digital images of freshwater green microalgae. The goal is to obtain representative algae shapes to extract morphological features to be employed in a posterior step of taxonomical classification of the species. The proposed methodology relies on the seeded region growing principle and on a fine-tuned filtering preprocessing stage to smooth the input image. A contrast enhancement process then takes place to highlight algae regions on a binary pre-segmentation image. This binary image is also employed to determine where to place the seed points and to estimate the statistical probability distributions that characterize the target regions, i.e., the algae areas and the background, respectively. These preliminary stages produce the required information to set the homogeneity criterion for region growing. We evaluate the proposed methodology by comparing its resulting segmentations with a set of corresponding ground-truth segmentations (provided by an expert biologist) and also with segmentations obtained with existing strategies. The experimental results show that our solution achieves highly accurate segmentation rates with greater efficiency, as compared with the performance of standard segmentation approaches and with an alternative previous solution, based on level-sets, also specialized to handle this particular problem.

Index Terms—Seeded region growing, freshwater green microalgae, image segmentation, Gaussian distribution

1 Introduction

Algae are a food source and primordial oxygen producers in aquatic environments, thus affecting water properties such as color, odour and taste [1]. Due to their sensitivity to environmental changes, these microorganisms act as effective indicators of water quality and ecological conditions. Researchers have been studying the potential of microalgae as biomass [2] or protein sources [3], in chemical processes [4], in oil production [5], and in medicine [6].

There exists a large number of microalgae species and families worldwide, and their taxonomical classification is a highly relevant problem in phycology. Recent taxonomical studies of freshwater green microalgae revealed an unknown diversity, especially in the *Selenastraceae* family, already acknowledged as possessing a highly problematic taxonomy [7] [8]. Findings on the real diversity of *Selenastraceae* resulted from phylogenetic studies on the sequencing data of the genes coding for 18S rDNA [8]. Traditional taxonomical classification that relies on analyzing morphological characteristics of specimens collected "in the field" is highly problematic, due to the subjective nature of the features considered and the wide morphological variety of algae shapes, which may be revealed only in cultured strains. For example, the presence of the pyrenoid, a feature considered for differentiating among species, sometimes can only be observed through electron microscopy. In some cases it may appear or not in a particular species depending on the conditions of the culture. The genomical studies indicated that morphologically similar strains may be molecularly very distinct, and also the opposite, with molecularly similar strains showing diverse morphology. Experts recognize that current knowledge on the specific diversity and ecology of the *Selenastraceae* on a worldwide scale is limited. For further genomical studies to be successful in clarifying the many pending issues, it is important to establish a common taxonomical basis using traditional approaches. Thus, it is important to improve the effectiveness of current practices adopted for analyzing morphological properties.

The taxonomical classification of freshwater green microalgae strains is often carried out manually by an expert. The procedure requires sampling algae cultures for observation under a microscope and then categorizing the observed organisms according to a predefined set of so-called "identification keys" which essentially contemplate their morphological features as their life cycle develops. This is a highly complex and time consuming process, demanding a detailed manual analysis of multiple images in order to identify the distinguishing features of the various species. Furthermore, the accuracy of a suggested taxonomical classification is highly dependent on the taxonomist's training and expertise. Even for experts, the task may prove difficult and error prone, as some algae species share similar morphological features, rendering their proposed classification inherently inaccurate.

There has been previous efforts towards developing computational support for taxonomical classification of algae species. Typically, the systems embed image processing

- *Vinicius R. P. Borges and Maria Cristina F. de Oliveira are with the Instituto de Ciências Matemáticas e de Computação, University of São Paulo (USP), São Carlos, SP, Brazil*
  E-mail: { viniciusrpb, cristina } at icmc.usp.br
- *Bernd Hamann is with the Department of Computer Science, University of California, Davis (UC Davis), Davis, CA, 95616, United States*
  E-mail: hamann@cs.ucdavis.edu
- *Thaís G. Silva and Armando A. H. Vieira are with the Departamento de Botânica, Federal University of São Carlos, São Carlos, SP, Brazil*
  E-mail: thais.garcia.bio@gmail.com,ahvieira@ufscar.br

Manuscript received April 19, 2005; revised September 17, 2014.

and pattern recognition algorithms that capture the relevant image properties and derive an appropriate representation for further processing. Nonetheless, some systems [9] [10] employ computationally expensive manual or user-guided segmentation procedures that render them difficult to use and unfeasible to handle larger image sets. Thus, the problem of how to extract representative information from green algae images with minimum user effort and maximal accuracy is still open.

In this paper we address this problem, focusing on strategies for automatically and accurately segmenting algae regions from microscope images, a necessary initial step to support the subsequent extraction of the shape features required for further taxonomical classification tasks. Segmentation must be highly precise, so that no fine detail is missed that may be relevant to distinguish between species in further classification stages. Algae cell structures, such as mucilage and concavities are fundamental to recognize specific algae species, and a highly accurate segmentation favors representative feature extraction and more precise taxonomical classification.

Image segmentation partitions a digital image into its disjoint constituent regions that share homogeneous properties (color or texture) and are expected to characterize the target objects [11] [12]. The problem is particularly challenging in images depicting samples from the *Selenastraceae* green algae family, due to peculiarities resulting both from the application domain and the image acquisition process (detailed in Section 2.2).

From the wide diversity of image segmentation methods, thresholding, edge-based and region-based strategies have been employed to segment biological images acquired with a microscope, such as phytoplankton [13], diatoms [14] and related algae genera [15]. Some authors adopted edge-based methods which search for image discontinuities characterized by abrupt intensity changes among regions [16]. Generally, these approaches compute derivatives between neighboring points in the image domain and select the higher responses, which are associated with edges. Conventional edge operators such as Roberts, Sobel and Prewitt [12] or the Canny edge detector [17] are popular choices. However, edge-based methods are sensitive to noise and require additional postprocessing steps to obtain regions with closed contours.

Methods based on dynamic curves that evolve towards image objects boundaries, such as Active Contours [18] and Level Set [19] [20] have also been successfully applied in this context. In a previous research, we combined a level set approach with automatically extracted edge and region information to guide the curve evolution towards the algae region boundaries [21]. Although it achieves good segmentation accuracy, the method suffers from a known limitation of contour-based approaches in general: it requires numerically solving Partial Differential Equations (PDEs), yielding a time consuming segmentation process unfeasible for real-time applications [22]. Moreover, it does not perform well on images of certain algae species with transparent areas.

Region-based methods, on the other hand, work by partitioning the image into multiple disjoint regions. A classical example is the Seeded Region Growing (SRG) algorithm proposed by *Adams and Bischof* [23]. The underlying rationale is, given a set of seeds (an image domain point or subregion), to grow regions by merging points with their nearest neighboring seeded region that satisfies a predefined homogeneity criterion. A criterion is chosen by taking into account the distinguishing characteristics of the multiple image regions. Region growing is effective, fast, robust to noise and requires no complex parameter tuning [24]. However, the suitable number of seed points, their placement in the image domain and the homogeneity criteria that characterize the image regions must be informed [11].

We exploit the region growing principle and a homogeneity criterion of image regions to introduce a specialized methodology to handle the described segmentation problem. Images are initially preprocessed for noise supression and then transformed to the Hue-Saturation-Value (HSV) space in order to reduce the intensity variation in their regions. After that, we perform a contrast enhancement in the hue channel using an equalized version of the value channel. A pre-segmentation image is automatically generated from the original RGB image that enables to define the proper number of seed points, avoiding undesirable situations of missing relevant regions or placing multiple seeds in a single region. The pre-segmentation image is also used to sample intensities of the algae and background regions in order to estimate their associated Gaussian distributions. The region homogeneity criterion to guide region growth is set by performing likelihood tests on the estimated Gaussian distributions. Finally, algae regions are smoothed with a morphological operation based on the rolling ball operator [25]. These steps compose a highly accurate and efficient technique for segmenting green algae images.

This paper is organized as follows: Section 2 presents similar region-based approaches for segmenting algae and biological images and establishes the motivation for this work. Section 3 describes the preprocessing steps for contrast enhancement and image smoothing. Section 4 details the proposed method, including the computation of the pre-segmentation image used in the sampling procedure and to obtain the seed points. Section 5 presents experimental results obtained by applying the proposed strategy to a set of green algae images. Finally, Section 6 provides conclusions and discusses possible future research.

2 Related Work and Motivation

The quality of segmentation directly affects the ability of successfully performing feature extraction from images. Defining an appropriate segmentation technique is a highly application dependent problem that requires a solid knowledge about specific image properties such as brightness, noise, texture and contrast. In the next sections we review related work from the literature and their limitations in face of the challenges identified for the green algae images, and describe the specific issues involved when segmenting algae images of the *Selenastraceae* family.

2.1 Previous work on microalgae segmentation

Over the last two decades many approaches have been introduced to identify or explicitly segment cells, objects or regions of interest in biological images. Most techniques

reported in the literature also detail preprocessing and post-segmentation procedures, since raw biological images are naturally noisy or present low contrast.

Edge-based segmentation methods based on identifying abrupt intensity changes are often employed in this context. Differential operators such as Sobel, Canny and Laplacian of Gaussian are typically combined with thresholding or the Wathershed transform [26] [27] to improve the accuracy of edge detection. *Jalba et al.* [28], for example, introduced a hybrid strategy that combines edge and region information to automatically segment diatoms. Their solution combines the Watershed transform and a mathematical morphology operation to select markers (small groupings of pixels). In order to avoid over-segmentation, a known drawback of the watershed method, a specific case of the Image Foresting Transform (IFT) is employed to change the image homotype. A final segmentation is obtained by extracting the external contour of the diatoms in the resulting watershed image. The method by Jalba et al. produced up to 98% correct contours. The failure cases were registered on diatom images with low contrast or blurred objects due to low resolution.

Mosleh et al. [29] developed a computer-based system to automatically detect, recognize, and identify specific microalgae species. Segmentation is based on detecting region boundaries with the Canny filter. However, the approach requires performing an edge linking in the resulting binary images for a correct identification of the algae's external closed contours. Then, essential morphological operations such as image border removal, boundary area filling and exclusion of small regions are performed on the binary images to preserve the algae regions only.

Promdaen et al. [30] proposed an automated methodology for microalgae classification which also includes preprocessing, segmentation and feature extraction steps. Specifically, segmentation can be performed in a single or in a multiresolution fashion, according to the morphological characteristics of the algae, determined during the process. The single approach is useful for algae shapes with subtle details and it is based on edge detection by the Canny filter. The multi-resolution part consists of running the single approach several times and incorporating additional steps to smooth the region boundaries.

Accurate segmentation based on edge detection requires object boundaries to be closed, otherwise further processing procedures are necessary, such as edge-linking. Contour-based approaches [18] [31] [21] based on dynamic curves can minimize such limitations, but depend on computing numerical solutions and on the convergence of an optimization process. In our previous research [21] we developed a specialized level set methodology that considers a statistical description of the algae and the background regions by means of Gaussian distributions. Although it achieves good segmentation accuracy, the method is computationally expensive, since it depends on the convergence of an optimization process. Another weakness of that method is related to the preservation of certain peculiar structures that appear in some specific algae species, such as mucilage.

Alternatively, region-based approaches rely on grouping neighboring pixels into regions according to a similarity criterion. Region growing algorithms have been applied to blood cell images [32], digital mammography [33], retinal vessel segmentation [34] and remote sensing [35]. Some authors have focused on developing application-specific approaches for automatic seed placement and the similarity decision strategy.

A marine phytoplankton identification system developed by *Cuiping et al.* [36] segments algae cells with a region-growing algorithm. First a Canny edge detector is applied to the original image to detect algae boundaries, followed by a morphological operator to remove small regions. Thresholding with Otsu's method is then applied to obtain a background patch for which a mean intensity value is estimated. The region-growing method uses intensities from a coarse background as a stopping criterion to automatically distribute the seeds through the image domain.

Tan et al. [37] proposed an automated system for marine algae identification which comprises the steps of filtering, segmentation, feature extraction and classification of species. First, a preprocessing step is required to highlight the presence of algae, due to the low contrast of the original images. A histogram of the corresponding HSV model is analyzed to decide whether to use green or white color for the threshold-based binarization. After the segmentation, a morphological operation attempts to fill holes and remove isolated microregions.

Schulze et al. [38] devised an automated system for phytoplankton recognition named *PlanktoVision*, which integrates image acquisition, segmentation, feature extraction and the classification process. Preprocessing consists of contrast adjustment by means of histogram normalization and boundary enhancement with the Sobel operator to handle transparency. Segmentation is based on region growing, in which the seeds are computed and placed through the background region using a rough segmentation obtained with the Watershed Transform. The mode values of each area in this segmentation are computed and the differences in their standard deviations are used to determine whether to merge similar regions.

Despite being successful on the applications to which they have been designed, the above methods cannot handle the specific challenges faced in the segmentation of images depicting algae from the *Selenastraceae* family, as detailed in the next section.

2.2 Problem characteristics

The images available to us confirm that the algae species from the *Selenastraceae* family are of diverse shapes, e.g., from round-shaped single cells, as illustrated in Figure 1(a), to the elongated organisms shown in Figure 1(b). Furthermore, the morphology of the algae may change along their life cycle. Some species remain solitary, others form colonies (grouped cells) which may also be very diversely shaped, as depicted in Figures 1(c) and 1(d).

Such natural diversity in addition to other peculiar image characteristics resulting from the acquisition process render the automatic segmentation of these images a very difficult task. Thus, a segmentation method which is shown to be effective on these samples is likely to perform well also on other samples depicting less complex microalgae families, providing an essential tool for further developments in the computational support to the taxonomical classification task.

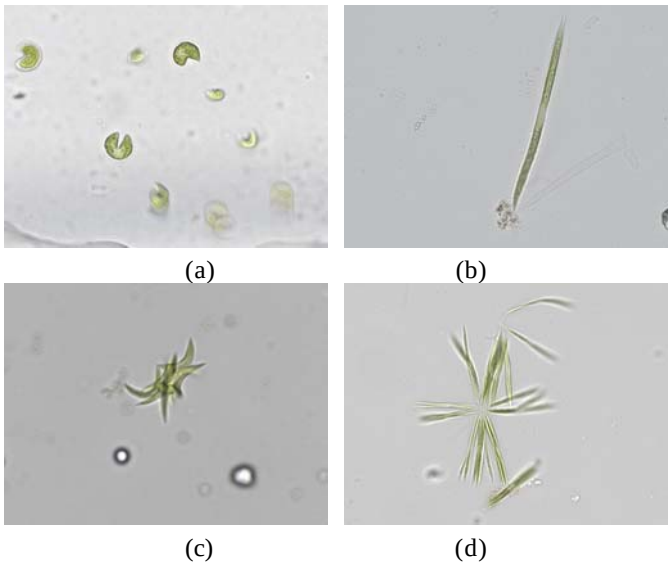

Fig. 1. Examples of green microalgae images: (a) image characterized by the presence of noise, artifacts and small objects; (b) elongated single algae image characterized by the mucilage in its bottom corner; (c) image depicting colonies where multiple algae cells overlap; (d) a colony of multiple elongated cells.

The images are acquired in the microscope with a resolution of 600×800 and are quantized in 8 bits per color channel. Each image depicts one or multiple algae regions, but they are all from a single species, as the image captures an observation of a specific cultured strain under the microscope. Notice how the intensities in the background regions of the multiple images in Figure 1 differ, and how each image shows a slight and smooth variation in its background. Moreover, although algae cells are generally green, they sometimes present brighter regions near corners (see Figures 1(c) and 1(d)) due to the algae's movement under the microscope lens.

The images also present noise and artifacts, for example, the image in Figure 1(a) shows some dark particles and an artifact in the bottom area. In Figure 1(b) we notice a transparent dead cell membrane touching the algae, surrounded by bright pixels, which will likely affect a shape detection procedure. Figure 1(c) presents round-shaped objects with bright interior and dark boundaries. Thus, the proposed segmentation methodology must be robust to noise and to the presence of artifacts.

To further illustrate the complexity of the segmentation task in this case, Figure 2 shows some segmentation results obtained with standard approaches from the literature that have been previously applied to biological images. We performed a binarization on the green channel of the original RGB image shown in Figure 1(d), using a threshold value computed with Otsu's method [39], which produced the image shown in Figure 2(a). The poor segmentation results are due to the wide range of intensities found in the interior of algae regions.

Alternatively, applying the Canny Edge detector to the green channel of the image in Figure 1(d) generates the binary image shown in Figure 2(b). Noticeably, the contours detected are not closed. The abrupt changes in intensities in the algae regions prevent the method from obtaining closed and regular contours.

In Figure 2(c) we present a segmentation result obtained with the Watershed Transform applied to the smooth image shown in Figure 2(a), in which we selected manually the area corresponding to the algae region in the watershed image. This result is affected by the smooth intensity variation in the background and the transparencies in the algae corners, which lead to poor segmentation because some algae areas could not be correctly recognized.

Figure 2(d) shows the segmentation produced by the level set approach introduced in our previous work [21], which did not manage to group some colony cells due to the presence of transparent areas, specifically in the regions where the algae cells meet. Thus, the diffusion process, inherent to the level set equation and responsible for smoothing the image, was not capable of suppressing the noise and handling the transparent regions, due to limitations of the RGB color model.

In the next sections we detail our novel approach to handle the segmentation. By changing the image representation to the HSV model and applying an appropriate contrast enhancement to highlight the critical areas we can improve segmentation accuracy and preserve the intricate shape properties of these microalgae species.

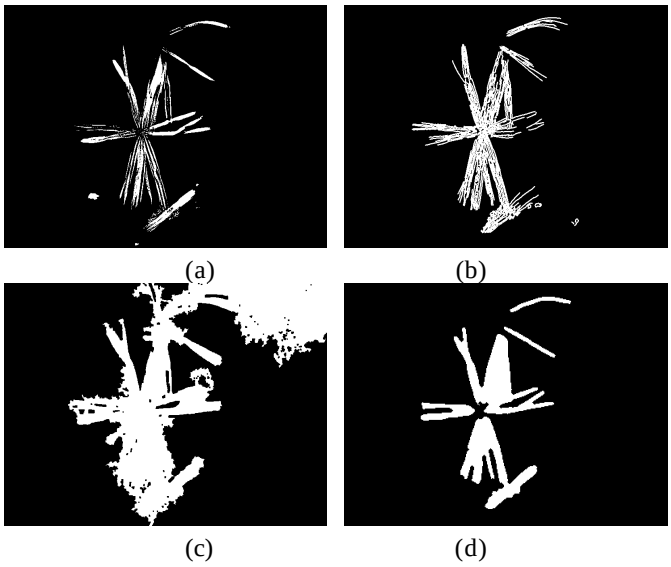

Fig. 2. Conventional approaches for segmenting biological images: (a) result obtained with binarization using Otsu's threshold; (b) result obtained with edge detection using the Canny algorithm; (c) result obtained with the Watershed Transform; (d) result obtained by an approach based on level set [21].

3 Preprocessing Steps

Some preprocessing steps are executed to improve image quality before applying the region growing algorithm. The first step smooths the original RGB image prior to obtaining its corresponding HSV representation. Further processing is applied to the Hue channel of the HSV representation, which provides sufficient contrast to distinguish between the algae and the background regions. A contrast enhancement is then applied to generate a smooth image with highlighted algae regions.

3.1 Image Smoothing

The original RGB image is initially filtered to suppress noise and artifacts observed in regions describing both algae cells and background. Smoothing is also important because the curves defining the algae cell boundaries are naturally rough and the pixel values in their internal regions are considerably heterogeneous, with colors varying from green to white.

In order to obtain smoother images in which both background and algae regions present homogeneous intensities, from a wide diversity of possible image filtering techniques we chose to apply the anisotropic diffusion filter (ADF) introduced by *Barcelos et al.* [40], because its smoothing process blurs the internal regions of the image while preserving boundary information.

Let $\Omega \subset \mathbb{R}^2$ be the image domain and $I : \Omega \rightarrow \mathbb{R}^3$ the function designed to describe a digital color image. The mathematical model for the ADF filter is given by:

$$u_t = g|\nabla u| div\left(\frac{\nabla u}{|\nabla u|}\right) - \lambda(1-g)(u-I), \qquad (1)$$

in which div is the divergence operator, $I = I(\boldsymbol{x})$ is the image to be filtered and $u = u(\boldsymbol{x}, t)$ is a smooth version of I at a time step $t > 0$, where $u(\boldsymbol{x}, 0) = I(\boldsymbol{x})$. The parameter λ balances the smoothness of the region boundaries – the goal is to smooth the boundary whilst preserving the important shape properties. g is a positive boundary potential, usually chosen as a decreasing function of the image gradient. This function must satisfy $\lim_{s\rightarrow\infty} g(r) = 1$, so that the diffusion process is reduced on the boundaries. Thus, a usual choice for g is given by:

$$g(r) = \frac{1}{1+|\nabla r|^2}. \qquad (2)$$

Eq. (1) is solved numerically by computing the Euler-Lagrange equations associated with a gradient descent scheme [41]. The partial differential equations obtained are discretized using the Finite Difference Scheme [42]. In order to compute the numerical solution for u, the parameters in Equations (1) and (2) were set to $\lambda = 0.01$ and $t = 20$ time iterations. These values were determined after experimenting with multiple combinations of parameter values, picking those values which yielded the best segmentation accuracy rates on a test data set. In the subsequent steps we shall denote the filtered image I_{ADF} as the final u.

Figure 3 illustrates this filtering process applied to an original green algae image, shown in Figure 3(a). The image smoothing result is presented in Figure 3(b), in which algae and background regions are more homogeneous as their edge information are preserved.

3.2 Obtaining the pre-segmentation image

In this step, we compute a pre-segmentation image using the eigenvalues of the covariance matrix of the filtered RGB image. This binary image provides a mask useful to identify the target foreground and background regions, which is necessary to compute the region seeds in the image domain and to delimit the region of interest for the enhancement process.

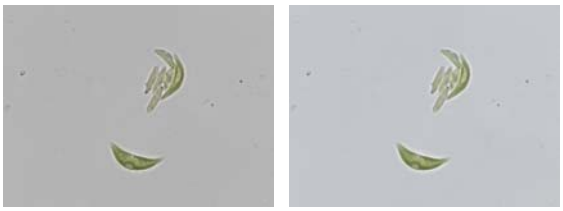

(a) (b)

Fig. 3. Anisotropic diffusion filtering: (a) original RGB image; (b) smooth image I_{ADF}.

First, we compute the local mean values μ_L relative to each point in the image domain $\boldsymbol{x} \in \Omega$:

$$\mu_L(\boldsymbol{x}) = \frac{1}{|\Omega|}\int_{\Omega} I(\boldsymbol{x}-\boldsymbol{y})d\boldsymbol{y}. \qquad (3)$$

$$A(\boldsymbol{x}) = I(\boldsymbol{x}) - \mu_L(\boldsymbol{x}). \qquad (4)$$

Then a local covariance matrix $C(\boldsymbol{x})$ of the color channels relative to each domain point is computed, given by:

$$C(\boldsymbol{x}) = A(\boldsymbol{x})^T A(\boldsymbol{x}). \qquad (5)$$

Finally, the eigenvalues and eigenvectors of the covariance matrix $C(\boldsymbol{x})$ are computed:

$$V^{-1}C(\boldsymbol{x})V = D, \qquad (6)$$

in which V is the matrix of eigenvectors and D is a diagonal matrix of the eigenvalues of $C(\boldsymbol{x})$, given by $v = \{D_{1,1}, ..., D_{m,m}\}$. The eigenvalues, which are computed for each pixel, can be represented as m images, each one capturing the image properties from a different perspective. An inspection of these eigenvalue images substantiated our choice of picking the third eigenvalue image (the green channel), which was the most effective to capture the algae characteristics.

It is possible to obtain a binary mask B_M that flags the pixels as associated with either algae or background regions by thresholding the third eigenvalue image using its mean intensity value. As a result, the algae-related pixels are one-valued in B_M, whereas the background pixels are assigned zero values. Finally, an erosion morphological operation is performed in B_M aiming to remove false responses that might arise on the background.

Figure 4 illustrates the process of obtaining the binary mask B_M departing from the smooth image depicted in Figure 3(b). Figures 4(a), 4(b) and 4(c) depict the images constructed from the first, second and third eigenvalues of each image domain point. After selecting the third eigenvalue image and thresholding it by its mean intensity value, the binary mask B_M shown in Figure 4(d) is obtained.

The pre-segmentation image B_M is then used in some further stages of the proposed methodology: in the region sampling procedure, to determine the seed points for each target region and to delimit the regions of interest for the enhancement process.

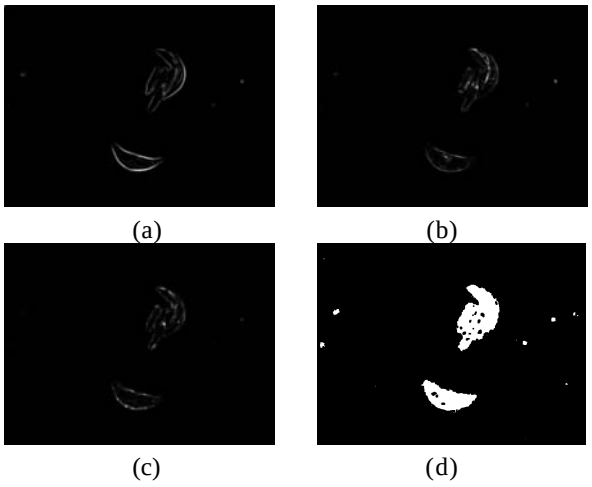

Fig. 4. Illustration of the steps in the computation of the binary mask: (a-b-c) the images representing the computed eigenvalues; (d) the pre-segmentation image obtained after thresholding the third eigenvalue image by its mean intensity value.

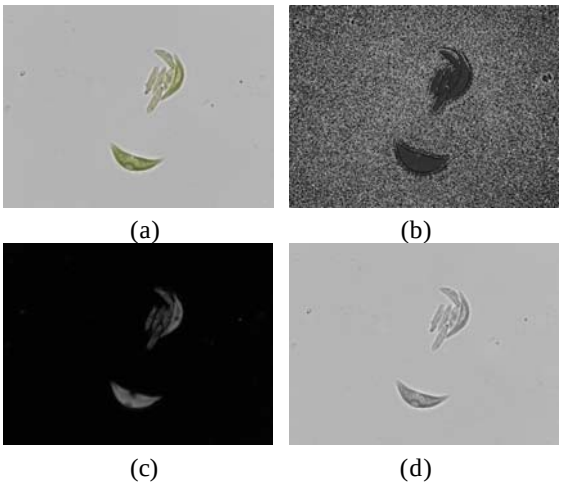

Fig. 5. Green algae image transformed to the HSV representation: (a) original RGB image; (b) Hue channel; (c) Saturation channel; (d) Value channel.

3.3 HSV Model

We chose to work with the HSV representation of the filtered RGB image I_{ADF}, which is more effective in capturing the contrast between the algae cells and the background.

The corresponding HSV model of a given RGB input image may be computed using the equations given in [12]. Figure 5 illustrates the results of the conversion for a particular green algae image. Figure 5(a) presents the original RGB image, whereas Figures 5 (b), (c) and (d) show the Hue (H), Saturation (S) and Value (V) channels of the corresponding HSV image. It is noticeable in the image showing the Hue channel, depicted in Figure 5(b), that the algae cells are characterized by a uniform gray intensity, whilst the background is noisy - it is possible to observe the lighting variation in the background areas. The saturation channel, shown in Figure 5(c), presents the algae regions in brighter intensities with blurred boundaries and it is discarded in the subsequent steps. The V channel image depicted in Figure 5(d) is simply a grayscale image, and is used in the following step responsible for the Hue contrast enhancement.

3.4 Image Enhancement

A contrast enhancement procedure is applied to the Hue channel in order to enable a more accurate identification of the algae regions. The procedure considers the intensity information registered in the Value channel, since the Hue channel alone may not disclose sufficient information. The rationale is to perform a histogram equalization in the Value channel that makes possible the analysis of the intensity variation of the background pixels and then identifying those intensity levels most likely associated with algae pixels. Such intensities are determined by thresholding the equalized image, thus generating a binary image that is used to weight and highlight the algae pixels in the Hue channel.

The histogram equalization generates a new image by quantizing the intensities in the Value channel to a predefined number of discrete gray levels. The pixel values are roughly uniformly distributed across the quantized gray level bins in image I_{EQ}, such that the resulting histogram is approximately flat. We chose to transform the value channel to 64 intensities for better discrimination of algae-related pixels, obtaining the equalized image I_{EQ}.

The algae regions are generally associated with the lower intensities in the histogram of image I_{EQ}. As the idea is to obtain a binary image that flags the algae-related pixels for enhancement, the threshold value τ is determined by considering the associated intensities in the histogram and the perimeter of the candidate algae regions in the pre-segmentation image. A histogram analysis revealed that the histogram of I_{EQ} has non-zero values at levels 1, 5, 9 and 12. However, gray level frequencies are highly dependent on the number of pixels that belong to algae regions. Thus, we binarize the equalized image I_{EQ} accordingly using the larger perimeter p from the candidate algae regions in the pre-segmentation image. The value of τ is determined as:

$$\tau = \begin{cases} 1, & \text{if } p \leq 500 \\ 5, & \text{if } p \leq 1000 \\ 9, & \text{if } p \leq 1500 \\ 12, & \text{otherwise.} \end{cases} \tag{7}$$

Once τ is obtained, the binary image B_{EQ} is computed as:

$$B_{EQ}(\boldsymbol{x}) = \begin{cases} 1, & \text{if } I_{EQ}(\boldsymbol{x}) \geq \tau \\ 0, & \text{otherwise,} \end{cases} \tag{8}$$

where B_{EQ} is the binary mask image flagging the algae-related pixels. The image enhancement will weight such pixels to emphasize their intensities, while preserving background patterns. This operation takes into account the perimeter p, since for images containing small or thin algae the Hue channel has typically low contrast due to an unbalanced amount of background pixels. Eq. (9) describes the enhancement process for algae images with $p > 250$, which doubles the intensities of the background pixels in the Hue channel I_{hue}:

$$I_H(\boldsymbol{x}) = \begin{cases} 2I_{hue}, & \text{if } B_{EQ}(\boldsymbol{x}) = 1 \\ I_{hue}, & \text{otherwise.} \end{cases} \quad (9)$$

When $p < 250$, we set $I_H = I_{hue} + B_{EQ}$ once the Hue channel does not present a high contrast between algae and background regions.

The intermediate image I_H in the above equation refers to the updated Hue channel with the algae regions highlighted. Finally, I_H is normalized to $[0, 1]$ resulting in the final enhanced image I_{EN}, which displays a better visual contrast between the algae and the background regions, as compared to the original hue channel. The steps of the enhancement procedure are illustrated in Figure 6. Figure 6(a) shows the original Hue channel image. Figure 6(b) presents I_{EQ}, the Value channel image after histogram equalization, in which the pixels associated with the algae cells have the lowest intensities. Figure 6(c) shows the weighted image B_{EQ} that indicates which pixels must be enhanced in the Hue channel. Finally, Figure 6(d) depicts the final enhanced Hue channel image, in which the algae regions are noticeably emphasized whereas the intensity patterns have been preserved.

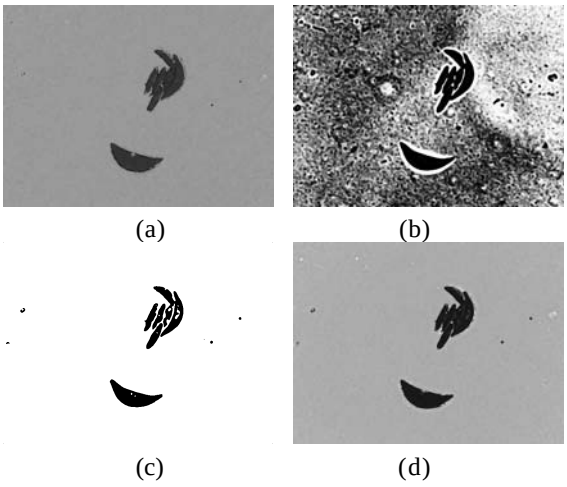

Fig. 6. Image enhancement: (a) the hue channel image I_{hue}; (b) the equalized Value channel image I_{EQ}; (c) the binary image B_{EQ}; (d) the enhanced Hue channel image I_{EN}.

Once the preprocessing steps are finished, we obtain an appropriate Hue channel I_{EN} for the upcoming segmentation process, in which algae cells have distinct intensities relative to the background pixels.

4 Seeded Region Growing

The seeded region growing algorithm, or simply region growing algorithm, operates by grouping (i.e., growing) pixels or subregions into larger regions based on a predefined similarity criterion [12]. Some seed pixels are initially selected based on some criterion (e.g. color, intensity, or texture). Once the initial seeds are placed, the growth process seeks to obtain homogeneous image regions, i.e., it tries to find an accurate segmentation of the image into regions with the property that each connected component of a region contains exactly one of the initial seeds. The presence of noise may result in oversegmentation, which is typically handled with a subsequent region merging process.

Two major concerns must be handled when performing a segmentation based on region growing: where to place the initial seeds in the image domain and which homogeneity criterion should be adopted to characterize the image regions. As for the seed placement problem, it is expected that segmentation of an image composed by N relevant target objects should start with N initial seeds, one located at each object. As for the region growing, the homogeneity criterion must capture the properties of the target objects.

For our specific problem, each relevant algae region (either a single cell or a colony) would require a seed representative. Thus, we devised an approach to automatically determine where to place the seed points, guaranteeing that one single seed will be placed in the interior of each algae region. The seed placement relies on a pre-segmentation image obtained from the filtered RGB image I_{ADF} (detailed in Section 3.2), which provides a binary mask useful to determine the seed points.

The homogeneity criterion and the conditional test to drive the region growth must account for the intensity variations of the algae pixels in the Hue channel. We chose to characterize the image regions (algae cells and background) by the Gaussian distributions of their intensities, described by their mean and standard deviation. These parameters are computed by automatically sampling a sub-set of pixels from each region. All the algae regions can be modeled with a single probability distribution, as the pixels associated with algae have the lowest intensities (darker regions) in the Hue channel.

Region Sampling

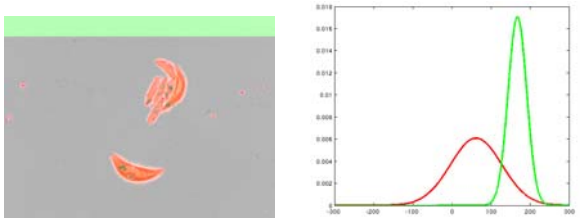

Fig. 7. Illustration of the region sampling procedure: (a) the red patches depict the algae region, while the green patch refers to the background region; (b) the estimated Gaussian distributions of the intensities in the algae (red line) and in the background (green line) regions.

The foreground and background regions in the image may be characterized by their intensity probability model distributions. The parameters characterizing the respective distributions may be estimated by sampling the foreground and background regions as identified in the pre-segmentation image B_M in the enhanced Hue image. The quality of the probability distribution estimation depends on an effective sampling procedure.

The sampling procedure is exemplified in Figure 7. Figure 7(a) illustrates the patches used to sample the target regions, namely the algae (shown in red) and the background (in green). For performance reasons, it is sufficient to sample only 10% of the background pixels. Figure 7(b) presents the estimated Gaussian distributions estimated for algae and background, given by their mean and standard deviations

as computed from the sampled intensities in their respective regions.

Setting the seeds

The pre-segmentation image possibly includes multiple algae regions, and it is necessary to determine manually a single pixel in each representative algae region. Artifacts characterized by small areas with less than 150 pixels may be found in these images, which must be disregarded. The principle is thus to consider individually each region (with area greater than 150 pixels) of B_M and select a contour point from an eroded version of B_M, thus making sure that the seed points are placed inside the target shapes.

Computing the seed points thus requires the following steps:

1) In an iterative process, perform successive morphological erosion operations on image B_M using a structuring element of size 1 until all regions completely shrink. Let n_I be the number of iterations performed.
2) Erode image B_M using a structuring element of size $\frac{n_I}{2}$, producing a new image B_{Er}.
3) Discard any regions in B_{Er} with perimeter smaller than 150 pixels.
4) Pick the top-leftmost pixel from the external contour of each region i in B_{Gr} as the respective region seed $(s_{i,1}, s_{i,2})$.

The above methodology guarantees that one seed is placed inside each algae region. The size of the structuring element was manually set by taking into account the image resolution and the algae area sizes. This process generates a set of seeds $\mathcal{S} = \{(s_{1,1}, s_{1,2}); ...; (s_{N,1}, s_{N,2})\}$ placed in the image domain for the region growing process.

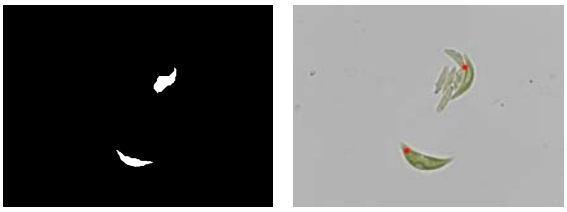

(a) (b)

Fig. 8. Determining the seeds: (a) the image B_{Er}; (b) the seed point placed over the algae region (shown in red).

Figure 8 illustrates the strategy for computing the seed points. Figure 8(a) shows the image B_{Er} resulting from executing Step 2 of the seed placement method. Figure 8(b) shows the seed point computed (shown in red) placed over the enhanced Hue channel image I_{EN}.

4.1 Homogeneity criterion

The homogeneity criterion defines whether a candidate pixel should be incorporated into a specific region. As such, it must consider the statistically relevant patterns of the different image regions, such as color, texture or intensity. Thus, a criterion must be chosen that captures the intensity patterns of the algae and the background regions.

In this case, the Gaussian distributions of the pixel intensities are effective to characterize the algae and the background regions in the Hue channel. First, the distributions parameters $\theta_1 = \{\mu_1, \sigma_1\}$ and $\theta_2 = \{\mu_2, \sigma_2\}$ are estimated, taking as parameters the means μ_i and the standard deviations σ_i computed from the algae and the background region samples, respectively, in the enhanced Hue image I_{EN}. Distributions P_1 and P_2 are thus computed as:

$$P_i(I(\boldsymbol{x})|\{\mu_i, \sigma_i\}) = \frac{1}{\sigma_i\sqrt{2\pi}} \exp\left(-\frac{||I(\boldsymbol{x}) - \mu_i||^2}{2\sigma_i^2}\right) \quad (10)$$

in which $||.||$ refers to the Euclidean norm. The distinctive Gaussian distributions of both regions are clearly depicted in the corresponding plots shown in Figure 7(b).

4.2 Region growth process

This process can be interpreted as a pixel labeling procedure in which all pixels belonging to a homogeneous region will be assigned the same label. The seed pixel is compared with its neighboring pixels, and they are grouped into a single region if the homogeneity criterion is satisfied. The region growing finishes once all pixels have been assigned a region label, which does not require a merging process.

Our implementation follows the region growing formulation described by *Gonzalez et al.* [12]. Let $\mathcal{S}$ be the set of seed points, in which $s_i \in \Omega$, and let P_1 (P_2) be the probability distribution associated with all the algae regions (background). Considering an 8-connectivity neighborhood, each image pixel is tested to verify whether it satisfies the criterion for inclusion in an algae region:

1) **IF** $P_1(I_{EN}(\boldsymbol{x})|\{\mu_1, \sigma_1\}) < P_2(I_{EN}(\boldsymbol{x})|\{\mu_2, \sigma_2\})$
2) **THEN** $\boldsymbol{x}$ belongs to an algae region;
3) **ELSE** $\boldsymbol{x}$ belongs to the background;

A binary image is obtained, where pixels that satisfy the conditional (domain points likely to belong to an algae region) are assigned a value 1, otherwise pixels are assigned a value 0. The next step relies on appending to each seed point in $\mathcal{S}$ all the one-valued points in the binary image which are 8-connected to it, resulting in an image with connected components corresponding to each algae cell, colony and background areas. In this process, we compute the probabilities of each neighbor pixel $\mathbf{y}$ and the region associated with a seed s:

$$d(\mathbf{y}) = |P_1(I_{EN}(\boldsymbol{y})|\{\mu_1, \sigma_1\}) - P_1(I_{EN}(s)|\{\mu_1, \sigma_1\})|. \quad (11)$$

Then $\mathbf{y}$ is grouped to the region associated to a seed s when condition $d(\mathbf{y}) < D_0$ is satisfied. D_0 is the average value of $d(\mathbf{y})$, that are the one-valued pixels in the pre-segmentation image B_M. Finally, each connected component receives a distinct region label, so that each algae region is uniquely identified. Additionally, a binary image B_{RG} is generated by keeping only the algae regions (as one-valued intensities) which are associated seed points.

Figure 9 illustrates the region growing process using the enhanced Hue channel image I_{EN} as input and the seed points indicated by the red marker in Figure 8(b). The result is shown in Figure 9(a), in which the white areas correspond

to pixels that are similar to the respective algae regions in terms of hue intensity.

(a) (b)

Fig. 9. Post-segmentation: (a) result of the region growing process for a particular image; (b) binary image representing the final segmentation, after applying the rolling ball.

4.3 Rolling ball transformation

The algae movement during the image acquisition leads to blurred corners and/or some transparent parts in the algae cells. As a result, in some cases the segmented algae shapes in B_{RG} might present small concavities and holes, as observed in the image depicted in Figures 9(a) and 10(a). This problem is handled by applying a rolling ball transformation to fill in any undesirable holes or concavities in the shapes obtained with the region growing process. The rolling ball operation produces another binary image I_{SEG} that denotes the final segmentation.

(a) (b)

Fig. 10. Rolling ball: (a) binary image resulting from the region growth process; (b) result obtained by the rolling ball.

The rolling ball transformation [43] can be described as a morphological closing of the target region, followed by a hole filling operation. A hole is a set of background pixels that cannot be reached by filling in the background from the edge of the image. In the rolling-ball transformation, a disk structuring element with a predefined radius is applied to the binary images.

Determining the size of the disk radius is difficult, since the algae shapes differ a lot in size and complexity. Setting a single radius size to handle all shapes would likely result in some poor quality segmentations.

We compute the radius size automatically for each case, taking into account the perimeter of the algae contours and some prior knowledge on their shapes. First, small algae do not require large disks for the rolling ball, because it is important to preserve their characteristic concavities. On the other hand, for algae colonies it is better to adopt medium-sized radii sizes, since the junctions between cells must be preserved. Finally, larger radius can be used on elongated algae shapes, which often present blurred corners and the rolling ball operation will not affect the shape essence, in this case.

Shape complexity is determined by identifying the number of peaks in its corresponding *Curvature Scale Space* (CSS) map [44]. The CSS descriptor captures the key local shape features by representing the shape boundary curvatures in a scale space which describes the locations of convex (or concave) segments and also detects the degree of convexity (or concavity) of such segments. The scale space representation of a shape is created by tracking the position of inflection points in a shape boundary filtered by low-pass Gaussian filters of variable widths. As the width of the Gaussian filter increases, negligible inflections are removed from the boundary and the shape becomes smoother. The remaining inflection points in the representation are likely to describe relevant object characteristics.

The result of this multi-scale smoothing process is a map depicting an interval tree formed by several inflection points. The shape contours have been subsampled to 200 points. Figures 11(a) and 11(b) show the CSS maps of the algae shapes depicted in Figures 9(a) and 10(a), respectively, in which the red points are the maxima. The $x-$axis presents the arc length of the algae contour after subsampling to 200 points. The $y-$axis refers to the width of the Gaussian low-pass filtering in the contour. It is noticeable that maps of colonies have more points of maximum than maps of single algae.

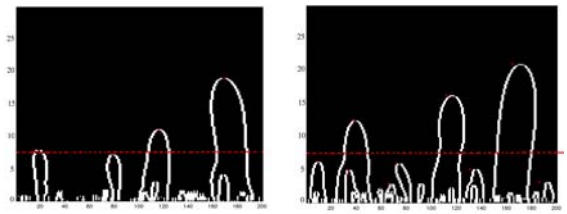

(a) (b)

Fig. 11. Curvature Scale Space maps: (a) map of the algae colony shape depicted in Figure 9; (b) map of the single algae shape depicted in Figure 10(b).

The number of peaks is identified by thresholding the CSS map at the Gaussian width 7, indicated in Figure 11 by the dashed red lines. Defining N_{CSS} as the number of peaks and p the shape perimeter, the disk radius is computed as:

1) **IF** $p > 250$ **AND** $N_{CSS} \leq 3$
2) **THEN** radius $\leftarrow 6$;
3) **ELSE** radius $\leftarrow 2$.
4) **END IF**

Figure 10(b) shows the result of applying the rolling ball operator to the binary image in Figure 10(a), in which holes and concavities were filled. Figure 9(b) presents the final segmentation result after the rolling ball transform produced smoother algae regions when comparing with the output image of the region growing, shown in Figure 9(a).

4.4 Segmentation pipeline

We can finally summarize the steps of the proposed segmentation framework:

- **Preprocessing**

1) The original RGB image I is filtered with the anisotropic diffusion filter, producing a filtered image I_{ADF};
2) The RGB image I_{ADF} is converted into its HSV representation, yielding the Hue, Saturation and Value channels;
3) The eigenvalue and eigenvectors of I_{ADF} are computed and a binary mask image B_M is composed;
4) An enhanced Hue channel image I_{EN} is obtained with contrast enhancement using B_M for the intensities adjustment;

- **Region growing process**

5) The binary mask B_M is used to place the seeds $\mathcal{S} = \{s_1, ..., s_N\}$ in I_{EN};
6) Pixel intensities from both the algae and background regions in I_{EN} are sampled using the binary mask B_M;
7) The Gaussian probability distributions parameters $\theta_1 = \{\mu_1, \sigma_1\}$ and $\theta_2 = \{\mu_2, \sigma_2\}$ are estimated from the algae and the background region samples, respectively.
8) The Gaussian distributions P_1 and P_2 of those regions are computed according to Eq. (10).
9) Region growing is applied to image I_{EN} using the set of seeds $\mathcal{S}$, the probability distributions P_1 and P_2, resulting in a binary image B_{RG} composed by the set of algae regions and background;

- **Post-segmentation**

10) The binary image B_{RG} is used as input to the rolling ball morphological operation to obtain the image I_{SEG}, which is the final segmentation.

In Section 5 we present results obtained from applying the above method and others from the literature on a particular set of green algae images.

5 Experimental Results

We evaluated the performance and the effectiveness of the proposed method on a set of 40 green algae images depicting different species of the *Selenastraceae* algae family complex. The experiments have been performed in a *Intel(R) Core(TM) i7 2.40GHz* and the MATLAB code is available for download [1]. For the sake of performance, in our implementation we analyse the green algae images considering individually each region of interest (algae regions identified by the seed points) in the region growing process.

The accuracy of the segmentation results obtained with our strategy and with methods from the literature are compared with manual segmentations of the images provided by the expert biologist, referred to as ground-truth (GT) images. For that purpose, region accuracy is measured with the Jaccard coefficient [45] and the F-Measure [46]. The F-Measure (F_1) is defined in terms of the precision (Pr) and the recall (Rc):

$$F_1 = 2\frac{Pr \;\; Rc}{Pr + Rc}. \tag{12}$$

Precision measures the percentage of region pixels in the automatic segmentation that correspond to region pixels in the ground-truth, being sensitive to over-segmentation. Recall measures the percentage of region pixels in the ground-truth that were detected via automatic segmentation, and is sensitive to under-segmentation. These measures are computed as:

$$Pr = \frac{TP}{TP + FP} \qquad Rc = \frac{TP}{TP + FN}, \tag{13}$$

where TP (true positive) refers to the pixels labeled as belonging to algae regions in both segmentation and GT. FP (false positive) refers to the pixels labeled as belonging to algae regions in the segmentation, but as non-algae pixels in GT. TN (true negative) refers to the pixels labeled as non-algae in both segmentation and in the GT. FN (false negative) refers to the pixels labeled as non-algae in the segmentation, but are actually pixels belonging to algae regions in the GT image. The F-Measure is the weighted average between precision and recall, in which F_1 values close to 1 indicate a high segmentation accuracy and 0 indicates lowest-possible segmentation accuracy.

The Jaccard coefficient (Jc) is defined as:

$$Jc = \frac{|I_S \cap I_{GT}|}{|I_S \cup I_{GT}|}, \tag{14}$$

in which $|\cdot|$ is the cardinality operator, I_S is the segmented image (binary image) and I_{GT} is the ground-truth image. The value of $Jc = 1$ when there is an exact match between the segmentation and GT, and $Jc = 0$ when a complete mismatch is observed. For both Jaccard coefficient and F-Measure, we compute the average accuracy for an image set by averaging the accuracy values computed for each image.

The proposed segmentation strategy is initially compared with three possible approaches: two of them are techniques commonly employed for segmenting biological images, namely the thresholding-based binarization with Otsu's automatic method for computing the threshold value, and the Watershed transform. The third technique is a specialized level set implementation targeted at the same problem of segmenting green algae images [21].

To ensure a meaningful comparison, the input images to the four segmentation approaches are the smoothed original images, resulting from applying the ADF filter with the same parameter settings and the rolling ball transformation in all cases to the initial segmentation results. The segmentations obtained with the Watershed transform required some additional postprocessing, as the method outputs multiple subareas. The relevant algae region is selected from the set of subareas by determining the seed points with the approach described in Section 4 and identifying the subareas that include the seed points.

Table 1 presents the computed mean accuracy rates and the standard deviations (std) for our method and the comparison techniques for the test image set. Moreover, the average running times (in seconds) are presented to compare the practical performance against the previous segmentation solution based on the level set approach. The Region

1. https://github.com/viniciusrpb/regiongrowing

Growing framework introduced in this paper yielded higher accuracy rates. This is mainly due to the appropriate design of the preprocessing and postsegmentation steps, as well as the usage of Gaussian distributions to characterize the target regions. The standard deviation (std) rates also suggest that it is more consistent, obtaining satisfactory segmentations in most test cases. We also observed that the segmented algae shapes are highly similar to the ground truth images.

TABLE 1
Average accuracy rates and execution times.

Segmentation techniques	Jc	F_1	time (s)
1. Region Growing framework	$\mathbf{0.77}$	$\mathbf{0.88}$	49.0
2. Specialized level set [21]	0.72	0.82	253.2
3. Binarization using Otsu's threshold	0.44	0.55	$\mathbf{1.2}$
4. Watershed transform	0.53	0.61	22.1

The running times in seconds (s) of each technique (shown in Table 1) indicate that the level set based approach requires more time to obtain the final segmentation. This can be explained by the underlying optimization process required to compute the numerical solution of the PDEs associated to the level set equation. In general, if a level set curve converges after k iterations, the overall algorithm complexity is denoted according to the big-O notation by $O(mnk)$, in which m and n are the dimensions of the input image. On the other hand, as the region growing methodology follows the implementation proposed by *Gonzalez et al.* [12], the complexity of the growing process is $O(Nmn)$, in which N is the number of seeds. As k is likely to be higher than N, the complexity of the level set approach is higher when compared to the adopted implementation of the region growing algorithm.

In the following analysis we detail the method's performance for some complex segmentation cases. We show the initial RGB image, the segmented image and also the images output by the preprocessing and the postsegmentation steps, due to their relevance to the process. In each case, the difficulties faced when segmenting such images are also discussed and visually illustrated.

The image in Figure 12 shows an algae colony, which poses a particular challenging segmentation case. Because the organisms are typically moving when the digital image is captured, the color intensity of algae cells vary considerably. The original image is shown in Figure 12(a); notice how the areas where the different cells meet are nearly transparent. Figure 12(b) shows the equalized image obtained during the contrast improvement of the hue channel. The enhacement process produces the new Hue channel shown in Figure 12(c). The image resulting from the region growing algorithm is presented in Figure 12(d), and Figure 12(e) shows the final segmentation, in which several holes were successfully filled by the rolling ball operator. Figure 12(f) depicts the associated ground-truth. The "star" shape of the colony has been very well preserved in the segmentation, which attained accuracy rates $F_1 = 0.85$ and $Jc = 0.74$.

Another segmentation case concerns an elongated algae cell which shows mucilage in the bottom corner. Handling the mucilage correctly is difficult. Ideally, it should remain connected to the algae cells, as it is characteristic of this kind of algae. However, conventional segmentation approaches

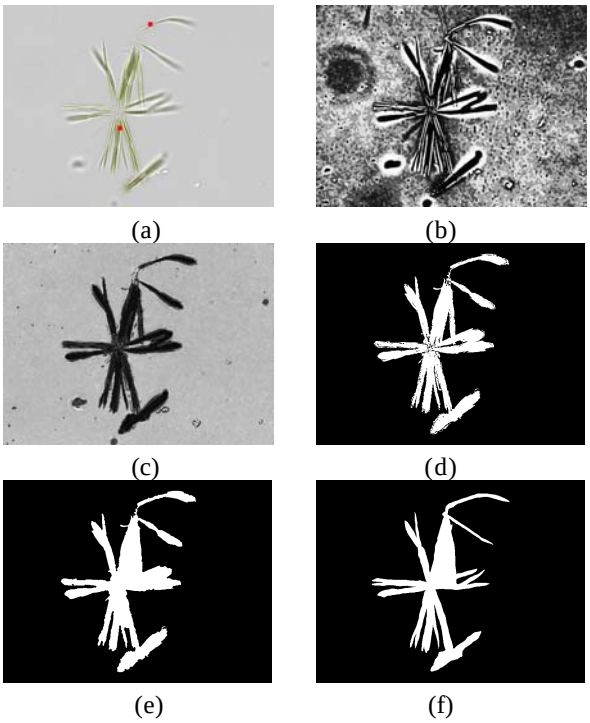

Fig. 12. Segmentation of an algae colony: (a) original RGB image (seeds denoted by the red points); (b) the equalized image I_{EQ} determined during the enhancement process; (c) enhanced Hue channel after contrast enhancement; (d) output of the region growing algorithm; (e) result after applying the rolling ball operator; (f) ground-truth image.

will very likely separate the structures. Figure 13 (a) depicts the original RGB image with a single algae and the obtained seed point (in red). Figure 13(b) shows the Hue channel, which is pretty noisy in this case. The smoothing and the enhancement processes produce an image with homogeneous regions and improved contrast between algae and background, shown in Figure 13(c). The final segmentation is presented in Figure 13(d), and the ground-truth is shown in Figure 13(e). Again, the algae cell shape including its particular mucilage was very well preserved, with segmentation accuracy rates $Jc = 0.85$ and $F_1 = 0.92$. Figure 13(f) presents the result of our previous level set approach, which shows the algae organism without its distinguishing mucilage structure.

We now analyze a particular case of the segmentation results obtained with the method proposed in this paper in comparison with those obtained with the Otsu's threshold binarization, the Watershed transform and our own previous attempt using a specialized level set approach [21]. The original image, depicting a single algae with its computed seed point (in red), is illustrated in Figure 14(a), whereas Figure 14(b) shows the manual segmentation generated by the biologist. Figure 14(c) replicates the segmentation result obtained with our method. Figures 14(d), 14(e) and 14(f) illustrate the results obtained, respectively, with the binarization approach, the adapted the Watershed transform and the specialized level set approach.

The segmentation obtained with the proposed region growing strategy is clearly most similar to the ground-truth, with segmentation accuracies given by $F_1 = 0.90$ and $Jc = 0.82$. The segmentation obtained with the thresholding-

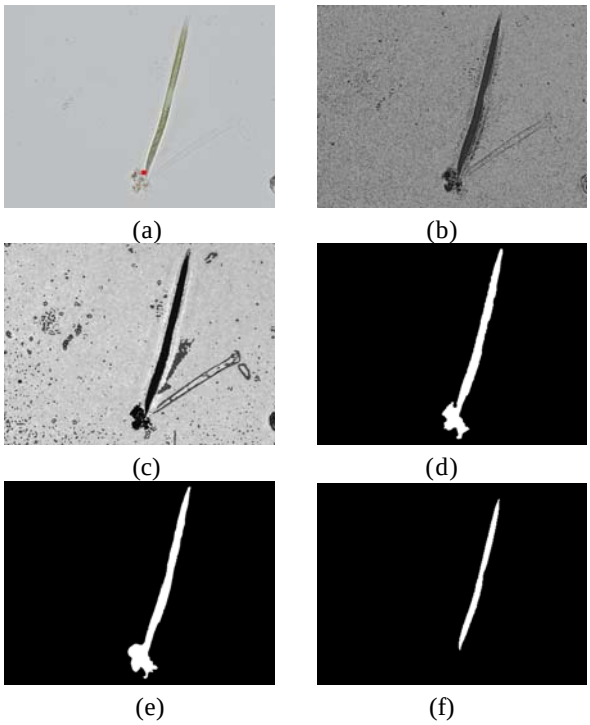

Fig. 13. Segmentation of an elongated algae cell: (a) original RGB image and its seed (in red) overplaced to the cell; (b) original Hue channel; (c) enhanced Hue channel; (d) segmentation after application of the rolling ball operator; (e) ground-truth image; (f) obtained resulting using the previous method [21].

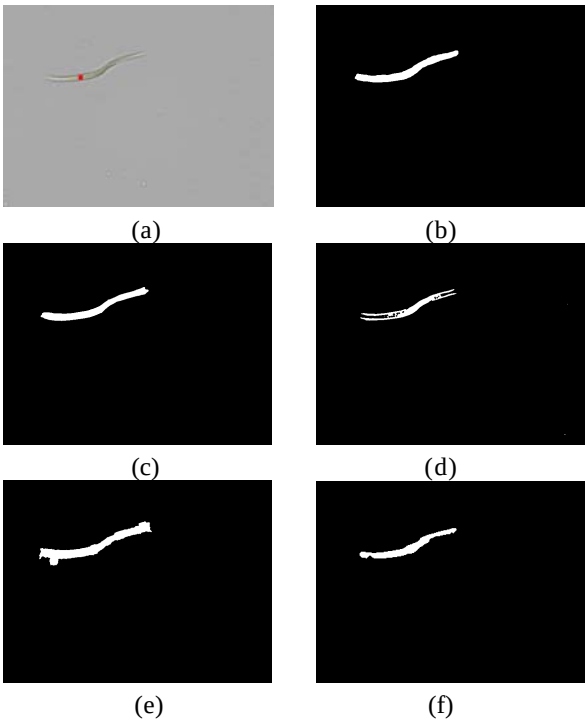

Fig. 14. Comparing results from different segmentation techniques: (a) original RGB image with seed (in red) overplaced to the cell; (b) ground-truth image; (c) segmentation with the proposed region growing method; (d) segmentation with thresholding; (e) segmentation with the Watershed method; (f) segmentation with a specialized level set approach [21].

based method deformed the original algae shape (accuracy rates are $F_1 = 0.71$ and $Jc = 0.55$). The Watershed based method achieved accuracy rates $F_1 = 0.70$ and $Jc = 0.75$ in this case, but the binary region presents a rough contour, even though the shape properties are well preserved. The specialized level set also output a highly accurate segmentation ($F_1 = 0.88$ and $Jc = 0.79$), but still inferior to the region growing, besides being more time consuming.

In Figure 15 we illustrate that the proposed segmentation methodology is also applicable to other types of digital microalgae images that share similar characteristics to the *Selenestraceae* images. Figure 15(a) presents the original RGB image of *Micrasterias pinnatifida* algae, in which the obtained seeds are shown by the red points. Figures 15(c) and 15(d) show the original hue channel and the enhanced hue image obtained with the same enhancement process applied to the *Selenastraceae* images, respectively. Figure 15(d) depicts the final binary image obtained after the region growing and the rolling ball procedures. One notices that the proposed method also works well on other types of algae images, but target cells should be green.

As reported elsewhere [21], the Gaussian distributions estimated using the HSV color space images can statistically characterize the target image regions effectively. The figures depicting the Hue channel images reveal target regions with a wide variety of patterns, which are well captured by the respective Gaussian distribution models. The pre-segmentation image provides the input to the region sampling procedure, ensuring a correct sampling of the representative intensities of each target region. The proposed solution also benefits from the pre-segmentation image both

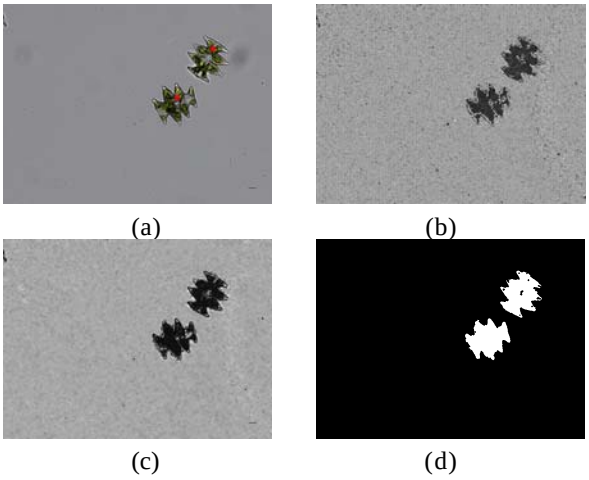

Fig. 15. Segmentation of *Micrasterias pinnatifida* in a microscopy image: (a) original RGB image; (b) original hue channel; (c) enhanced hue channel; (d) the final segmentation.

to determine a single seed point for each region and to ensure that they are correctly placed inside algae regions.

Beyond its higher segmentation accuracy rates, the new method can naturally handle noise and artifacts, and also treat the variability observed in the hue channel and the pre-segmentation images. Small noisy signals are disregarded when computing the seed points, so that only the relevant algae regions are kept in the final segmentation. This is a major advantage over our previous results obtained on this image collection with a modified level set approach [21],

which departs from the assumption that any boundary information potentially describes an algae region. Furthermore, the current method is computationally more efficient than the level set approach, which depends on the convergence of the dynamic contour.

A limitation that remains to be further investigated concerns the detection of transparent algae cells, since neither the pre-segmentation image nor the enhancement process could correctly identify the algae shapes in these cases, hampering the subsequent steps of intensity sampling and seed point placement. In this situation, the intensities of the algae regions and the background are very similar. Thus, edge-based methods are likely to perform better, since they can still detect the algae boundaries in these adverse conditions.

6 Conclusion

In this paper we presented a methodology for segmenting green microalgae images based on the region growing principle and incorporating specific smoothing and contrast enhancement steps. The image regions, i.e., the algae cells and the background, are described by Gaussian distributions computed prior to the region growing, estimated by means of region intensity samples. The rationale for generating this representation is to capture the subtle intensity variations observed in algae cells for accurate segmentation.

Segmentation is performed in the Hue channel, which is effective in capturing the contrast between algae and background regions. Each seed point for region growing is associated with a specific region and the growth process groups neighboring pixels that satisfy a predefined homogeneity criterion characterizing the image regions. We also introduce a strategy for computing a binary image from the original RGB, useful to automatically determine the seed points and to obtain patches for the region sampling procedure.

Experimental results have shown that the proposed method achieves high segmentation accuracy when compared with ground-truth segmentations provided by the biologists. Moreover, it also yielded better accuracy rates than existing methods from the literature, such as segmentation with the Watershed transform, binarization using Otsu's technique, and a specialized level set method devised for green algae images.

Our next goal is to extract morphological features from the green algae from the segmented shape properties, in order to provide computational support for taxonomical classification of these particularly challenging algae species.

Acknowledgment

The authors acknowledge the support from the State of Sao Paulo Research Funding Agency (FAPESP) grants 2011/22749-8, 2012/00269-7, 2013/26647-0) and the Brazilian Federal Funding Agency (CNPq) grant 305696/2013-0.

References

[1] P. McCormick and J. Cairns, "Algae as indicators of environmental change," *Journal of Applied Phycology*, vol. 6, no. 5, pp. 509–526, 1994.

[2] A. Demirbas, "Use of algae as biofuel sources," *Energy conversion and management*, vol. 51, no. 12, pp. 2738–2749, 2010.

[3] E. W. Becker, "Micro-algae as a source of protein," *Biotechnology advances*, vol. 25, no. 2, pp. 207–210, 2007.

[4] K. Skjånes, C. Rebours, and P. Lindblad, "Potential for green microalgae to produce hydrogen, pharmaceuticals and other high value products in a combined process," *Critical reviews in biotechnology*, vol. 33, no. 2, pp. 172–215, 2013.

[5] M. Shiho, M. Kawachi, K. Horioka, Y. Nishita, K. Ohashi, K. Kaya, and M. M. Watanabe, "Business evaluation of a green microalgae botryococcus braunii oil production system," *Procedia Environmental Sciences*, vol. 15, pp. 90–109, 2012.

[6] M. Soheili and K. Khosravi-Darani, "The potential health benefits of algae and micro algae in medicine: a review on spirulina platensis," *Current Nutrition & Food Science*, vol. 7, no. 4, pp. 279–285, 2011.

[7] L. Krienitz, I. Ustinova, T. Friedl, and V. A. R. Huss, "Traditional generic concepts versus 18s rrna gene phylogeny in the green algal family selenastraceae (chlorophyceae, chlorophyta)," *Journal of Phycology*, vol. 37, no. 5, pp. 852–865, 2001.

[8] M. W. Fawley, M. L. Dean, S. K. Dimmer, and K. P. Fawley, "Evaluating the morphospecies concept in the selenastraceae (chlorophyceae, chlorophyta) 1," *Journal of phycology*, vol. 42, no. 1, pp. 142–154, 2006.

[9] K. Embleton, C. Gibson, and S. Heaney, "Automated counting of phytoplankton by pattern recognition: a comparison with a manual counting method," *Journal of Plankton Research*, vol. 25, no. 6, pp. 669–681, 2003.

[10] S. Brasch, L. Linsen, and G. Fuellen, "Vanlo-interactive visual exploration of aligned biological networks," *BMC Bioinformatics*, vol. 10, no. 1, p. 327, 2009.

[11] S. C. Zhu and A. L. Yuille, "Region competition: unifying snakes, region growing, energy/bayes/mdl for multi-band image segmentation," *IEEE Transactions on Pattern Analysis and Machine Intelligence*, vol. 18, pp. 884–900, 1996.

[12] R. C. Gonzalez, *Digital image processing*. Pearson Education India, 2009.

[13] H. M. Sosik and R. J. Olson, "Automated taxonomic classification of phytoplankton sampled with imaging-in-flow cytometry," *Limnology and Oceanography: Methods*, vol. 5, no. 6, pp. 204–216, 2007.

[14] I. Dimitrovski, D. Kocev, S. Loskovska, and S. Džeroski, "Hierarchical classification of diatom images using ensembles of predictive clustering trees," *Ecological Informatics*, vol. 7, no. 1, pp. 19–29, 2012.

[15] H. Zheng, H. Zhao, X. Sun, H. Gao, and G. Ji, "Automatic setae segmentation from chaetoceros microscopic images," *Microscopy research and technique*, vol. 77, no. 9, pp. 684–690, 2014.

[16] S. Gupta and S. G. Mazumdar, "Sobel edge detection algorithm," *International journal of computer science and management Research*, vol. 2, no. 2, pp. 1578–1583, 2013.

[17] J. Canny, "A computational approach to edge detection," *IEEE Transactions on Pattern Analysis and Machine Intelligence*, no. 6, pp. 679–698, 1986.

[18] M. Kass, A. Witkin, and D. Terzopoulos, "Snakes: Active contour models," *International Journal of Computer Vision*, vol. 1, no. 4, pp. 321–331, 1988.

[19] S. Osher and J. A. Sethian, "Fronts propagating with curvature-dependent speed: algorithms based on hamilton-jacobi formulations," *Journal of Computational Physics*, vol. 79, no. 1, pp. 12–49, 1988.

[20] R. Malladi, J. A. Sethian, and B. C. Vemuri, "Shape modeling with front propagation: A level set approach," *IEEE Transactions on Pattern Analysis and Machine Intelligence*, vol. 17, no. 2, pp. 158–175, 1995.

[21] V. R. P. Borges, B. Hamann, T. G. Silva, A. A. Vieira, and M. C. F. Oliveira, "A highly accurate level set approach for segmenting green microalgae images," *28th Conference on Graphics, Patterns and Images (SIBGRAPI)*, pp. 87–94, 2015.

[22] M. Emmett and M. Minion, "Toward an efficient parallel in time method for partial differential equations," *Communications in Applied Mathematics and Computational Science*, vol. 7, no. 1, pp. 105–132, 2012.

[23] R. Adams and L. Bischof, "Seeded region growing," *IEEE Transactions on Pattern Analysis and Machine Intelligence*, vol. 16, no. 6, pp. 641–647, 1994.

[24] J. Fan, G. Zeng, M. Body, and M.-S. Hacid, "Seeded region growing: an extensive and comparative study," *Pattern Recognition Letters*, vol. 26, no. 8, pp. 1139 – 1156, 2005.
[25] S. Lou, X. Jiang, and P. J. Scott, "Applications of morphological operations in surface metrology and dimensional metrology," *Journal of Physics: Conference Series*, vol. 483, no. 1, p. 012020, 2014.
[26] K. Haris, S. N. Efstratiadis, N. Maglaveras, and A. K. Katsaggelos, "Hybrid image segmentation using watersheds and fast region merging," *IEEE Transactions on Image Processing*, vol. 7, no. 12, pp. 1684–1699, 1998.
[27] L. J. Belaid and W. Mourou, "Image segmentation: a watershed transformation algorithm," *Image Analysis & Stereology*, vol. 28, no. 2, pp. 93–102, 2011.
[28] A. C. Jalba, M. H. F. Wilkinson, and B. T. M. Roerdink, "Automatic segmentation of diatom images for classification," *Microscopy Research and Technique*, vol. 65, no. 1, pp. 72–85, 2004.
[29] M. A. Mosleh, H. Manssor, S. Malek, P. Milow, and A. Salleh, "A preliminary study on automated freshwater algae recognition and classification system," *BMC Bioinformatics*, vol. 13, no. Suppl 17, p. S25, 2012.
[30] S. Promdaen, P. Wattuya, and N. Sanevas, "Automated microalgae image classification," *Proc Computer Science*, vol. 29, pp. 1981–1992, 2014.
[31] S. Osher and R. P. Fedkiw, "Level set methods: an overview and some recent results," *Journal of Computational Physics*, vol. 169, no. 2, pp. 463–502, 2001.
[32] S. H. Shirazi, A. I. Umar, N. U. Haq, S. Naz, and M. I. Razzak, "Accurate microscopic red blood cell image enhancement and segmentation," *Bioinformatics and Biomedical Engineering*, pp. 183–192, 2015.
[33] T. Berber, A. Alpkocak, P. Balci, and O. Dicle, "Breast mass contour segmentation algorithm in digital mammograms," *Computer methods and programs in biomedicine*, vol. 110, no. 2, pp. 150–159, 2013.
[34] Y. Q. Zhao, X. H. Wang, X. F. Wang, and F. Y. Shih, "Retinal vessels segmentation based on level set and region growing," *Pattern Recognition*, vol. 47, no. 7, pp. 2437–2446, 2014.
[35] X. Zhang, P. Xiao, X. Feng, J. Wang, and Z. Wang, "Hybrid region merging method for segmentation of high-resolution remote sensing images," *ISPRS Journal of Photogrammetry and Remote Sensing*, vol. 98, pp. 19–28, 2014.
[36] S. Cuiping, Y. Chenhui, L. Huizhen, and K. Lin, "A system for identification of marine phytoplankton," *2nd International Conference on Signal Processing Systems*, vol. 3, pp. 423–426, 2010.
[37] C. S. Tan, P. Y. Lau, S.-M. Phang, and T. J. Low, "A framework for the automatic identification of algae (neomeris vanbosseae ma howe): U 3 s," *International Conference on Computer and Information Sciences (ICCOINS)*, pp. 1–6, 2014.
[38] K. Schulze, U. M. Tillich, T. Dandekar, and M. Frohme, "Planktovision–an automated analysis system for the identification of phytoplankton," *BMC Bioinformatics*, vol. 14, no. 1, p. 115, 2013.
[39] N. Otsu, "A threshold selection method from gray-level histograms," *Automatica*, vol. 11, no. 285-296, pp. 23–27, 1975.
[40] C. A. Z. Barcelos and V. Pires, "An automatic based nonlinear diffusion equations scheme for skin lesion segmentation," *Applied Mathematics and Computation*, vol. 215, no. 1, pp. 251–261, 2009.
[41] G. Aubert and P. Kornprobst, "Mathematical problems in image processing: partial differential equations and the calculus of variations," *Springer Science & Business Media*, vol. 147, 2006.
[42] W. F. Ames, *Numerical methods for partial differential equations*. Academic Press, 2014.
[43] S. R. Sternberg, "Grayscale morphology," *Computer Vision, Graphics, and Image Processing*, vol. 35, no. 3, pp. 333 – 355, 1986, special Section on Mathematical Morphology.
[44] F. Mokhtarian and R. Suomela, "Robust image corner detection through curvature scale space," *IEEE Transactions on Pattern Analysis and Machine Intelligence*, vol. 20, no. 12, pp. 1376–1381, 1998.
[45] F. Ge, S. Wang, and T. Liu, "New benchmark for image segmentation evaluation," *Journal of Electronic Imaging*, vol. 16, no. 3, pp. 0 330 111–03 301 116, 2007.
[46] S. Alpert, M. Galun, A. Brandt, and R. Basri, "Image segmentation by probabilistic bottom-up aggregation and cue integration," *IEEE Transactions on Pattern Analysis and Machine Intelligence*, vol. 34, no. 2, pp. 315–327, 2012.

Vinicius Ruela Pereira Borges received the B.Sc. and M.Sc. in computer science from the Federal University of Uberlândia, Minas Gerais, Brazil, in 2008 and 2011, respectively. He is currently a Ph.D. candidate at the University of São Paulo and has recently been a visiting researcher at University of California, Davis, USA. His main research interests are in image processing, pattern recognition and visual analytics.

Maria Cristina Ferreira de Oliveira is at the Computer Science Department, Instituto de Ciências Matemáticas e de Computação (ICMC), University of São Paulo (USP), Brazil. She received a B.Sc. in computer science from USP in 1985, and a Ph.D. degree in electronic engineering from the University of Wales, Bangor, UK, in 1990. Her current research interests are in data and information visualization, pattern recognition, visual analytics and visual data mining.

Thaís Garcia Silva received a bachelor degree in Biology from São Paulo State University, Brazil and Ph.D. degree in Sciences, focused on Ecology and Natural Resources from the Federal University of São Carlos, in 2009 and 2016, respectively. Her research interests include taxonomy, systematics and phylogeny of freshwater phytoplankton and diversity and biogeography of green algae.

Armando Augusto H. Vieira received the B.Sc. degree in Biology in 1972, the M.Sc. degree and the Ph.D. degree in Oceanography from São Paulo University, Brazil, in 1975 and 1980, respectively. He is now a professor at Federal University of São Carlos, Brazil. His research interests include the study of the functions of extracellular algal polysaccharides, freshwater microalgae culture collection and excretion of organic matter by freshwater algae.

Bernd Hamann teaches computer science at the University of California, Davis. He studied computer science and mathematics at the Technical University of Braunschweig, Germany, and he obtained a Ph.D. in computer science from Arizona State University, U.S.A. His main interests are data analysis and visualization, geometric design and modeling, and image processing.